Biochemical Pharmacology 226 (2024) 116383

Contents lists available at ScienceDirect

Biochemical Pharmacology

journal homepage: www.elsevier.com/locate/biochempharm

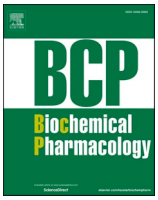

The short-chain fatty acid acetate modulates orexin/hypocretin neurons: A novel mechanism in gut-brain axis regulation of energy homeostasis and feeding

Nicola Forte [a], Brenda Marfella [a,b], Alessandro Nicois [a,c], Letizia Palomba [a,c], Debora Paris [a], Andrea Motta [a], Maria Pina Mollica [b,d,e], Vincenzo Di Marzo [f,*], Luigia Cristino [a,*]

[a] Institute of Biomolecular Chemistry, National Research Council of Italy, Pozzuoli, Naples, Italy
[b] Department of Biology, University of Naples Federico II, Naples, Italy
[c] Department of Biomolecular Sciences, University of Urbino Carlo Bo, Urbino, Italy
[d] Centro Servizi Metrologici e Tecnologici Avanzati (CeSMA), Complesso Universitario di Monte Sant'Angelo, 80126 Naples, Italy
[e] Task Force on Microbiome Studies, University of Naples Federico II, 80138 Naples, Italy
[f] Canada Excellence Research Chair on the Microbiome-Endocannabinoidome Axis in Metabolic Health, Faculty of Medicine and Faculty of Agricultural and Food Sciences, Université Laval, Québec City, QC, Canada

ARTICLE INFO

Keywords:
SCFAs
Hcrt
Obesity
Microbiota
Endocannabinoids

ABSTRACT

The short-chain fatty acids (SCFAs) acetate, propionate and butyrate, the major products of intestinal microbial fermentation of dietary fibres, are involved in fine-tuning brain functions via the gut-brain axis. However, the effects of SCFAs in the hypothalamic neuronal network regulating several autonomic-brain functions are still unknown. Using NMR spectroscopy, we detected a reduction in brain acetate concentrations in the hypothalamus of obese leptin knockout ob/ob mice compared to lean wild-type littermates. Therefore, we investigated the effect of acetate on orexin/hypocretin neurons (hereafter referred as OX or OX-A neurons), a subset of hypothalamic neurons regulating energy homeostasis, which we have characterized in previous studies to be over-activated by the lack of leptin and enhancement of endocannabinoid tone in the hypothalamus of ob/ob mice.

We found that acetate reduces food-intake in concomitance with a reduction of orexin neuronal activity in ob/ob mice. This was demonstrated by evaluating food-intake behaviour and orexin-A/c-FOS immunoreactivity coupled with patch-clamp recordings in *Hcrt*-eGFP neurons, quantification of prepro-orexin mRNA, and immunolabeling of GPR-43, the main acetate receptor. Our data provide new insights into the mechanisms of the effects of chronic dietary supplementation with acetate, or complex carbohydrates, on energy intake and body weight, which may be partly mediated by inhibition of orexinergic neuron activity.

1. Introduction

The bidirectional communication between the central nervous system (CNS) and the gastrointestinal tract, modulated by hormones and vagal afferents, results in an intricate anatomical-morpho-functional system that promotes or inhibits food-intake [1]. This interaction forms a network in which signals from the CNS influence the motor and secretory functions of the gastrointestinal tract, which in turn, affect cerebral functions [2,3]. Deregulation of this gut-brain axis contributes to the development of eating disorders [4] and metabolic diseases such as obesity [5]. The latter pathological condition is characterized by hyperleptinemia, an increase in peripheral and cerebral tissue inflammation, particularly in the hypothalamic region [6,7], and gut dysbiosis, a disruption of the taxonomic composition and function of the gut microbiota [8,9]. The gut microbiota supports gut-brain communication and contributes to many physiological processes by regulating, among others, immune system function and hormone secretion [10,11]. Obesity is accompanied by gut dysbiosis, with profound functional

Abbreviations: 2-AG, 2-arachidonoylglycerol; DSE, depolarization-induced suppression of excitation; DSI, depolarization-induced suppression of inhibition; eCB, endocannabinoid; eCBome, endocannabinoidome; HFD, high-fat diet; HCRT, Hypocretin; OX-A, orexin A; LH, Lateral Hypothalamus.

* Corresponding authors at: Institute of Biomolecular Chemistry, National Research Council of Italy, Pozzuoli, Napoli, Italy (Luigia Cristino); Universitè Laval, Quebec City, QC, Canada (Vincenzo Di Marzo).

E-mail addresses: vincenzo.dimarzo@criucpq.ulaval.ca (V. Di Marzo), luigia.cristino@icb.cnr.it (L. Cristino).

https://doi.org/10.1016/j.bcp.2024.116383
Received 3 June 2024; Received in revised form 19 June 2024; Accepted 20 June 2024
Available online 20 June 2024

changes in the metabolites produced by commensal microorganisms acting on the host [12]. Accordingly, faecal transplantation from obese mice and humans to germ-free mice has obesity-promoting effects [13], although the underlying mechanisms remain unclear [11,14].

The intestinal microbiota metabolize complex indigestible carbohydrates as a primary source of energy. The main products of this fermentative process are short-chain fatty acids (SCFAs) acetate, propionate, and butyrate. The molar ratio of these molecules in healthy rodents is 60:20:20 [15], making acetate the most abundantly produced SCFA in these animals. However, because of gut dysbiosis, profound changes in SCFA levels are found in both the feces and plasma of obese rodents [16,17].

Importantly, the absence and subsequent reintroduction of the gut microbiota in germ-free mice profoundly alters the levels of the lipid mediators and receptors belonging to another major player in energy metabolism and the gut-brain axis, the extended endocannabinoid (eCB) system, or endocannabinoidome (eCBome), in both the intestine and brain [18,19]. Accordingly, some of these mediators and receptors, including the eCBs anandamide and 2-arachidonoylglycerol (2-AG), and/or one of their main molecular targets, the CB1 receptor, are positively correlated with, or negatively regulated by SCFAs, in inflammatory conditions [20,21]; in contrast, the expression of eCB biosynthetic enzymes were found to be inhibited by SCFA-producing bacteria in epithelial intestinal cells [22].

Acetate has been reported to have opposing effects on appetite via the two G-protein-coupled receptors GPR41 (appetite stimulation) and GPR43 (appetite inhibition) [11]. However, data are lacking on the distribution of GPR41/GPR43 in the brain of lean and obese mice and the direct effect of acetate on the brain. Moreover, conflicting results have been reported on the association between acetate and obesity [11]. For example, some studies have indicated a positive correlation between faecal acetate concentrations and obesity, while others have demonstrated a negative relationship [23]. One study reported that acetate suppresses appetite by increasing pro-opiomelanocortin (POMC) mRNA in the hypothalamus [24] and exerts an anti-inflammatory effect that accompanies weight and visceral fat mass loss in male rats with high-fat-diet (HFD)-induced obesity [25]. However, another study showed that acetate induces overeating in rodents consuming an HFD by promoting hyperphagia and weight gain [26]. Contrasting results have also been reported in obese leptin knockout ob/ob mice, a genetic model of obesity that cannot produce leptin, where elevated or unchanged levels of acetate were found in the appendix compared to the same tissue of normal-weight mice [13,27].

The hypothalamus acts as a hub in the gut-brain axis, as it receives and integrates peripheral signals from the gastrointestinal tract as well as other brain regions, and modulates responses to appetite and food-intake [28]. Orexins (OXs, also called hypocretins, HCRTs) are neuropeptides found in two isoforms (OX−A and OX−B) and involved in several essential physiological functions, such as energy homeostasis, sleep-wake cycle, and somatic motor control [29]. OX-A and B are synthesized in neurons located exclusively in the lateral hypothalamus (LH) and projecting to several brain areas [30]. Orexin levels exhibit a robust diurnal fluctuation since they slowly increase during the dark period, or active phase (i.e., ZT13-24), and decrease during the light period, or rest phase (ZT0-ZT12), in the microdialyzed fluid collected from the LH in rodents, according to their physiological implication in arousal and wakefulness states [31].

In HFD and ob/ob obese mice, upregulation of OX signalling occurs, supported by factors such as impaired leptin signalling and subsequent excessive eCB levels and/or misplaced CB1 receptor localization. Indeed, acute or chronic deficiency of leptin signalling associated with fasting or severe obesity leads to activation of OX neurons with increased OX mRNA and protein levels [32,33]. On the other hand, it was demonstrated by our group and others that OX-A induces the biosynthesis of the eCB, 2-AG [34], which plays an important role as a potent modulator of synaptic transmission through activation of CB1 receptors by either enhancing or reducing excitatory or inhibitory drive on neurons, ultimately affecting their excitability [35]. The eCBs are synthesized following neuronal depolarization or metabotropic receptor activation of post-synaptic neurons and retrogradely activate CB1 receptors expressed at presynaptic terminals [35,36]. When CB1 receptors are activated in glutamatergic terminals, they trigger a depolarization-induced suppression of excitation (DSE), which causes a reduction in excitatory synaptic transmission. On the other hand, activation of CB1 receptors in GABAergic terminals leads to depolarization-induced suppression of inhibition (DSI), resulting in the decrease of inhibitory synaptic transmission [36,37]. Both these forms of synaptic plasticity have been shown to regulate OX-A release in different energy states [32,38]. Thus, eCB signalling at CB1 receptors, which is only one of the ways through which the larger eCBome participates in the control of food-intake, is regulated by, and in turn regulates, OX-A signalling in the hypothalamus and other brain areas.

Although a central role of OX neurons in the regulation of feeding behaviour [39] and the control of the gut-brain axis [40] has been demonstrated, data on the potential role of acetate in regulating OX neuron activity, and subsequently eCB levels, in the hypothalamus of lean and obese mice are lacking. To fill this knowledge gap and better understand the mechanisms behind the effect of acetate on appetite and energy homeostasis, we investigated here: (i) the effect of acetate on food-intake in Wt and ob/ob mice and on the functional activity of OX neurons; and (ii) the anatomical distribution and expression of the SCFA receptor GRP43 in the brain of Wt and obese mice before and after administration of acetate.

2. Materials and methods

2.1. Animals and drugs.

The experiments were carried out on 8- to 12-week-old male mice with spontaneous non-sense mutation of the ob gene for leptin (ob/ob, JAX mouse strain, B6.Cg-Lepob/J) and wild type ob gene expressing homozygous siblings obtained by breeding ob gene heterozygous mice and genotyping with PCR. In an experimental subset 8- to 12-week-old male Prepro-orexin-eGFP Tg(Hcrt-eGFP/Rpl10a) JD218Jdd were used.

All experiments were carried out according to the guidelines established by the European Communities Council (Directive 2010/63/EU of 22 September 2010) and approved by the Italian Ministry of Health (authorization n. 152/2020-PR and 589/2018). All the mice were housed under controlled temperature (20–23 °C) and humidity conditions (55 ± 5 %) and received standard chow ad libitum. All animals were used in scientific experiments for the first time and were not previously exposed to any pharmacological treatments. Each figure legend and statistical analysis indicates the number of mice used in each experiment. Since orexin levels exhibit a robust diurnal fluctuation (levels slowly increase during the dark period or active phase (i.e., ZT13-24) and decrease during the light period or rest phase, all the mice were housed under 12 h light:12 h dark cycle, light on at 8:00 PM, i.e. ZT0, and acetate (500 mg/kg) injected for 3 days every 12 h starting from ZT2 and the brain removed 1 h after the last injection for the biochemical NMR and immunohistochemical studies.

2.2. Food-intake measurements

Mice were isolated one per cage and fed ad libitum. Food-intake was measured for 2 days to obtain an average of the food consumed daily. To increase the motivation to eat during the test, lean and obese mice were subjected to 50 % caloric restriction the day before the test. During the first test session the mice were injected with a vehicle and 2 g of food were administered and the food-intake was assessed after 1 h, 2 h, and 4 h after acetate injection (500 mg/kg) at ZT2 [24].

2.3. NMR sample preparation and spectra acquisition

To extract the metabolites of interest, frozen brain tissues were mechanically disrupted. Then, the combined extraction of polar and lipophilic metabolites was carried out by using the methanol/water/chloroform protocol [41]. This procedure separates three phases: water/methanol at the top (polar fraction, containing polar metabolites), denatured proteins and cellular debris in the middle, and chloroform at the bottom (nonpolar fraction, containing lipophilic metabolites). Polar and nonpolar fractions were transferred into glass vials and the solvents were removed by using a rotary vacuum evaporator at room temperature and stored at −80 °C until measurements. For NMR analysis, the polar fractions were resuspended in 630 μl of phosphate buffer saline (PBS, pH 7.4), adding 70 μl of $^{2}H_2O$ solution [containing 1 mM sodium 3-trimethylsilyl [2,2,3,3-$^{2}H_4$] propionate (TSP) as a chemical shift reference for ^{1}H spectra] to provide a field frequency lock, reaching 700 μl of total volume. The samples were then transferred to NMR tubes for analysis. One-dimensional (1D) spectra were acquired at 600.13 MHz on a Bruker Avance III-600 spectrometer equipped with a TCI CryoProbeTM fitted with a gradient along the Z-axis, at a probe temperature of 27 °C, using the excitation sculpting sequence for solvent suppression [42]. Spectra were referred to internal 0.1 mM sodium trimethylsilylpropionate (TSP), assumed to be at $\delta = 0.00$ ppm. These 1D spectra were used for multivariate statistical analysis. In addition, two- dimensional (2D) clean total-correlation spectroscopy (TOCSY) and heteronuclear single quantum coherence (HSQC) experiments were acquired to help metabolite identification and signal assignment. 2D spectra were referenced to the lactate doublet assumed to resonate at $\delta = 1.33$ ppm for ^{1}H, and $\delta = 20.76$ ppm for ^{13}C. Metabolites were assigned to NMR profiles by comparison of chemical signal shifts (^{1}H and ^{13}C nuclei) with literature data [43] and/or an online database [44].

2.4. Hypothalamic quantitative RT-qPCR

This was carried out using the methods described by Bewick et al. [45]. Quantitative reverse transcriptase PCR (RT-qPCR) was used to study the expression of the different target genes. Total RNA was extracted from the whole hypothalami using TRIZOL (Invitrogen) according to the manufacturer's protocol. All samples were treated with DNaseI (Invitrogen) before the reverse transcription. First-strand cDNAs were prepared using 1 μg RNA and SuperScriptII Reverse Transcriptase (Invitrogen) in the presence of random hexamer and oligo(dT) primers (Promega, Charbonnières-les-Bains, France). The qPCRs were performed using the Light Cycler Fast Start DNA Master SyBR Green I kit (Roche, Meylan, France) in the presence of specific primer pairs selected to amplify small fragments (100–200 bp). PCR products were checked for specificity by measuring their melting temperature. Samples (in duplicate) were quantified by comparison with a standard curve obtained by dilutions of purified-specific cDNAs.

2.5. Measurements of POMC mRNA expression

RNA was extracted from the dissected hypothalamus using an Absolutely RNA micro prep kit from Stratagene (La Jolla, CA, USA). The gene transcription for POMC in the arcuate nucleus (ARC) of the hypothalamus was determined using real-time RT-PCR, and results were expressed as a ratio to the expression of the constitutive gene cyclophilin. The sequences of TaqMan probes and primers for cyclophilin (GenBank accession no. M15933) were: forward primer 5′-CCCACCGTGTTCTTCGACAT; reverse primer 5′-TGCAAACAGCTCGAAGCAGA-3′; and probe 5′-CAAGGGCTCGCCATCAGCCG-3′. The probe and primers for POMC (assay identification no. Rn00595020_ml) were purchased from Applied Biosystems.

2.6. Lipid extraction and endocannabinoids measurement

Tissue samples were pooled and analyzed using liquid chromatography–atmospheric pressure chemical ionization–mass spectrometry (LC-APCI-MS; LabSolution Shimadzu), The eCB 2-AG was extracted from tissues and then purified and quantified as previously described [46]. First, hypothalamic tissues were pooled and homogenized in 5 vol chloroform/methanol/Tris-Cl 50 mM pH 7.5 (2:1:1 by volume) containing 50 pmol of d5-2-AG as internal deuterate standard. Homogenates were centrifuged at 13,000 × g for 16 min (4 °C), and the aqueous phase plus debris were collected and four times extracted with 1 vol chloroform. The lipid-containing organic phases were dried and prepurified by open-bed chromatography on silica columns eluted with increasing concentrations of methanol in chloroform. Fractions for 2-AG measurement were obtained by eluting the columns with 9:1 (by volume) chloroform/methanol and then analyzed by LC-APCI-MS. LC-APCI MS analyses were carried out in the selected ion monitoring mode, using *m/z* values of 384.35 and 379.35 (molecular ions + 1 for deuterated and undeuterated 2-AG). 2-AG levels were therefore calculated based on their area ratios with the internal deuterated standard signal areas. Values are expressed as pmol per mg of wet tissue extracted.

2.7. Immunohistochemistry

Mice injected with acetate (i.p., 500 mg/kg every 12 h for 3 days starting from ZT2) were used for immunohistochemical studies. c-FOS immunohistochemistry was performed by following the analysis of the food-intake behaviours in mice after 1 h of acetate or vehicle injection (500 mg/kg) at ZT2.

Animals were euthanized under isoflurane anaesthesia and perfused transcardially with 0.1 M phosphate buffer saline (PBS) followed by 4 % paraformaldehyde in 0.1 M phosphate buffer (PB), pH 7.4. The brain was removed, fixed and cryoprotected with 30 % sucrose in PB. Brain sections were cut by Leica CM3050S cryostat into 10 μm-thick through the coronal plane, collected in three alternate series and maintained frozen until being processed immunofluorescence.

For immunofluorescence labelling, the brain sections were incubated overnight in a mixture of the following primary antibodies diluted in PB-T (0.3 % PB-Triton): goat anti-OX-A (1:100; SC-8070; Santa Cruz Biotechnology, Inc. Dallas, Texas – U.S.A.); rabbit anti-c-FOS (1:100; SC-52; Santa Cruz Biotechnology, Inc., Dallas, Texas); rabbit anti-GPR43 (1:100; bs-13536R; Bioss Inc, Beijing, China). Then the sections were treated for three hours with a mixture of appropriate Alexa anti-IgGs secondary antibodies (Invitrogen, ThermoFisher Scientific, France) diluted 1:50 in PB-T as Alexa-488 donkey anti-goat (A11055), Alexa-594 donkey anti-rabbit (A21207) and Alexa-488 donkey anti-rabbit (A21206). Sections were counterstained with DAPI (4′,6-diamidino-2-phenylindole) (Sigma-Aldrich S.r.l., Milan, Italy) to detect nuclei, and coverslipped with aqueous mounting medium Aquatex (Merck, Darmstadt, Germany).

Controls of immunolabeling specificity in multiple fluorescence experiments were performed by omission of primary or secondary antibodies or by pre-absorption of primary antibodies with the respective blocking peptides. Immunofluorescence was analyzed by the confocal microscopy Nikon Eclipse Ti2, and images were acquired with the digital camera DS-Qi2 (Nikon) and processed by Image analysis software NIS-Elements C (Nikon, Florence, Italy). N = 6–10 z-stacks were collected through each analyzed section every 0.5 μm throughout the area of interest to be processed by the MetaMorph imaging deconvolution software (Leica©, Germany). One focus image of serial Z plane for each channel was selected and merged to realize an optimal multichannel image. Micrographs were saved in TIFF format and adjusted for light and contrast before being assembled on plates. The brain regions of interest were identified by referencing the Allen Mouse Brain Atlas [47].

2.8. Analysis of the immunohistochemical experiments

For the quantitative evaluation of immunolabeling serial Z plane images were collapsed into two-dimensional images ($n \leq 30$ planes with an increment 0.5 μm). The initial parameters assessed included the measurement of the percentages of c-FOS co-localization in OX-A immunoreactive areas of LH, an unbiased physical dissector-based counting of double immunoreactive puncta performed following the protocols described in Bolte and Cordelières [48]. Additionally, we determine the percentage of GPR43-labeled cells in LH and around the 3 V, defined as the area expressing GPR34 immunolabeling. All analyses were conducted by an observer blinded to the experimental design.

2.9. Electrophysiological recordings

Tg(Hcrt-eGFP/Rpl10a)JD218Jdd 8–12 weeks old mice were deeply anesthetized with isoflurane and the brain was removed. LH containing coronal slices (250 μm) were cut using a Leica VT1000 S Vibrating blade microtome at 3–5 °C in a solution composed of (in mM): 87 NaCl, 25 $NaHCO_3$, 2.5 KCl, 0.5 $CaCl_2$, 7 $MgCL_2$, 10 glucose, 75 sucrose, and saturated with 95 % O2 and 5 % CO_2. After cutting, we let the slices recover 1 h at 37/38 °C and 30 min at RT in artificial cerebrospinal fluid (ACSF) containing in mM: 125 NaCl, 25 $NaHCO_3$, 10 glucose, 2.5 KCl, 1.25 NaH_2PO_4, 2 $CaCl_2$, and 1 $MgCl_2$ (bubbled with 95 % O_2-5 % CO_2). Coronal slices were transferred to a recording chamber and continually perfused with gassed ACSF. Hcrt-eGFP neurons were visualized using a 470 nm light source (CoolLED pE-100).

The recording was performed with a Multiclamp 700B/Digidata1440A system and a Leica DM6000 FS microscope equipped with a WAT-902H Ultimate camera. Pipette, pulled using a Sutter P-1000 puller, had a resistance of 3–7 MΩ when filled with ACSF/KCl or K-gluconate solution. Data were acquired at 10 kHz sample frequency and filtered at 2 kHz with a low-pass Bessel filter.

Spontaneous action potentials were detected in loose cell configuration in voltage clamp (0 mV) lowering the pipette on the neuronal surface and applying a small suction until the series resistance reached a 35–50 MΩ resistance. In an experimental subset the inhibitor of GPR43-GLPG0974 (Tocris) (100 nM) was used, while to inhibit CB1R was used AM251 (Tocris) at 4 μM. The inhibitory synaptic activity was recorded in whole cell patch clamp configurations (Vc = -60 mV) using a high chloride intracellular solution containing (in mM): 126 KCl, 4 NaCl, 1 $MgSO_4$, 0.02 $CaCl_2$, 0.1 BAPTA, 15 glucose, 5 HEPES, 3 ATP, and 0.1 GTP. pH 7.3 with KOH, 290 mOsm/L. Spontaneous inhibitory post-synaptic currents (sIPSCs) were recorded in the presence of 50 μM D-(2R)-amino-5-phosphonovaleric acid (D-APV) and 10 μM 6-cyano-7-nitroquinoxaline-2,3-dione (CNQX) (Tocris Bioscience, Ellisville, MO), to inhibit NMDA and AMPA receptors.

The excitatory synaptic activity was recorded using a K-gluconate-based intracellular solution containing (in mM): 126 Kgluconate, 4 NaCl, 1 $MgSO_4$, 0.02 $CaCl_2$, 0.1 BAPTA, 15 glucose, 5 HEPES, 3 MgATP, and 0.1 NaGTP, pH 7.3, 290 mosmol/L. Spontaneous excitatory post-synaptic currents (sEPSCs) were recorded in the presence of 30 μM Bicuculline, 5 μM CGP55845 (Tocris Bioscience, Ellisville, MO) to inhibit GABAA and GABAB receptors respectively.

Data were acquired with pClamp 10.4 software (Molecular Devices) and analyzed offline with Clampfit 11.2 (Molecular Device), Excel, and GraphPad Prism 8.0.2 (GraphPad Software, USA).

2.10. Analysis of electrophysiologic data

To analyze the variation of the firing rate in the presence of acetate we plot the firing rate relative to the baseline of 5–10 min calculated as 100 %. DSI and DSE were examined by recording spontaneous inhibitory post-synaptic currents (sIPSCs) and spontaneous excitatory post-synaptic currents (sEPSCs) respectively (Vc: −60 mV) for 10 sec. Subsequently, a depolarization step of 5 sec duration at 0 mV was applied to the recorded Hcrt-eGFP, followed by the sIPSCs recorded for 20 sec at −60 mV. We reported the percentage changes in frequency and amplitude from the baseline calculated in the 5 sec bin before and after the depolarization step.

2.11. Statistic

Statistical analysis was conducted using GraphPad Prism Software version 8.0.2. Tests were considered significant when $p < 0.05$. Data are presented as mean ± SEM. Sample sizes for experiments were determined based on those used in similar experiments previously reported in the literature. The data distribution was analyzed using the D'Agostino-Pearson test. One-sample t-tests were used to analyze comparisons of a single group relative to its baseline. For unpaired group comparisons, data were analyzed using a two-tailed Mann-Whitney *U* test. Paired group comparisons were analyzed using the Wilcoxon matched-pairs signed-rank test (two-tailed). When comparing three or more groups, data were analyzed using One-way ANOVA/Bonferroni, Kruskal–Wallis/Dunn's tests, or 2-way ANOVA with Sidak's post hoc.

3. Results

3.1. Acetate reduces food-intake less efficiently in ob/ob mice than in Wt mice

SCFA levels were measured by NMR-based analysis of hypothalamic brain extracts from adult Wt and ob/ob mice fed ad libitum. In line with the increment of acetate metabolism reported in the adipose tissue of obese mice [49,50], we observed a decrease of acetate concentrations in the hypothalamus of ob/ob mice compared with lean Wt control, although propionate concentrations remained unchanged in the same range, and butyrate was not detectable (Fig. 1**A and 1B**).

Caloric restriction reduces acetate levels [51], whereas acute intraperitoneal (i.p.) acetate injection reduces food-intake in lean mice [24]. To test if acetate (i.p. 500 mg/kg) produces an anorectic effect in obese ob/ob mice we measured food intake at 1, 2, and 4 h from acetate injection in ob/ob and Wt mice after overnight food deprivation.

We found a slight but non-significant tendency of ob/ob mice to eat more than Wt mice after vehicle injection (Fig. 1**C**). Acetate injection decreased food-intake in both Wt (Fig. 1**D**) and ob/ob mice (Fig. 1**E**). However, this effect lasted up to 4 h in lean Wt mice in comparison to 2 h in ob/ob mice (Fig. 1**F**), suggesting an increment of acetate degradation, or a reduction of its actions, in obese mice. Therefore, hypothalamic acetate concentrations were quantified by NMR-based analysis in vehicle- or acetate-treated mice after 1, 2 and 4 h from injection. An increase of acetate levels was found in the brain of Wt mice at 1 h and 2 h after acetate treatment, while no differences were observed in the obese mice at different time-point of acetate injection (Fig. 1**G**), indicating increased acetate degradation in ob/ob mice.

3.2. Acetate modulates c-FOS expression in orexin neurons, GPR43 expression and eCB levels in obese mice

Among the brain regions, the hypothalamus has the highest efficiency in acetate uptake [24]. Several mechanisms have been proposed to mediate the anorexic effect induced by acetate [24,25], but no data have been reported regarding the possible role of OX neurons. Consistent with previous observations reporting the enhancement of orexinergic activity in the brains of obese mice [32,33], here we observed increased c-FOS expression in OX-A neurons from ob/ob mice vs lean Wt mice (Fig. 2**A and 2B**). Injection of acetate (every 12 h for 3 consecutive days; 500 mg/kg i.p.[24]) reduced the percentage of c-FOS/OX-A immuno-coexpressing neurons in both Wt and ob/ob mice (Fig. 2**A and 2B**).

To investigate if acetate was able to affect OX-A neurons by acting at the selective SCFA receptors GPR43 [52] we performed an

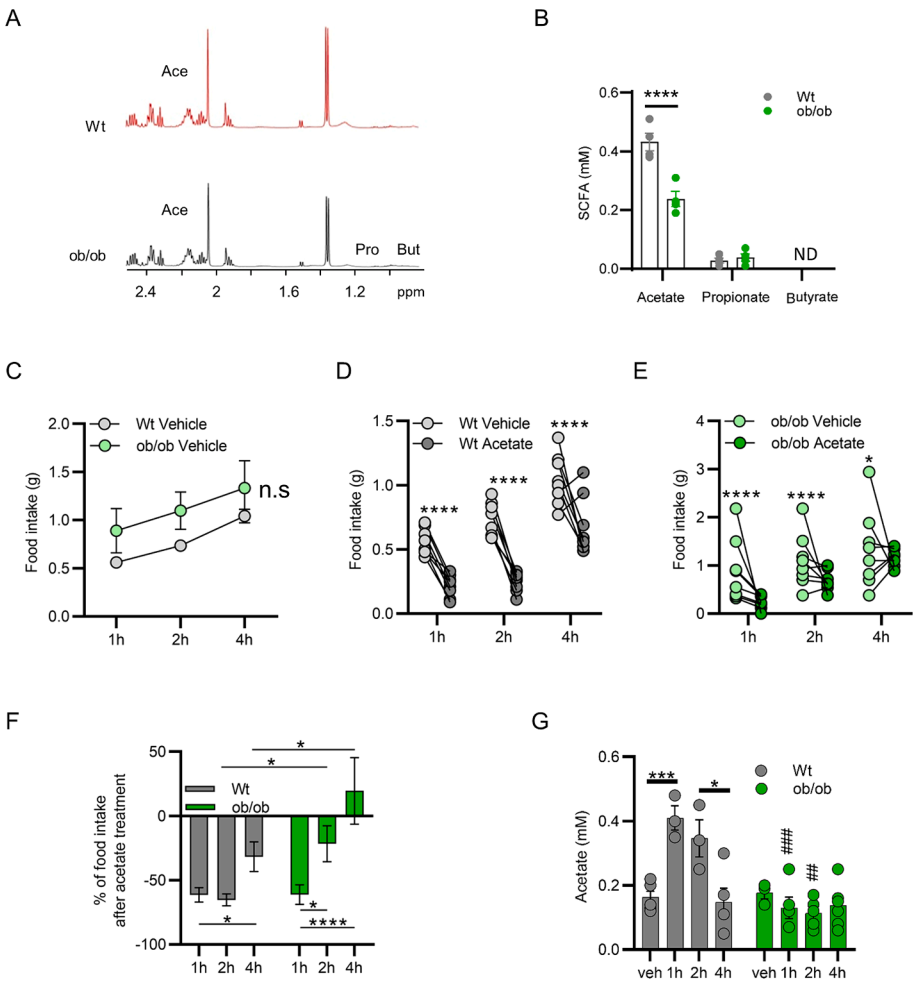

Fig. 1. Acetate is less effective at **reducing food-intake in ob/ob mice compared to Wt mice.** (**A**) 600-MHz NMR spectra of the high-field regions of the brain extract from Wt and ob/ob mice. The regions contain the acetate (Ace) signal; Pro, propionate and But, butyrate. (**B**) NMR quantitative analysis of SCFAs concentration in the hypothalamus of obese and Wt mice. ****, $p < 0.0001$, two-way ANOVA and Sidak's multiple comparisons test. (C) Data showing food-intake in Wt and ob/ob mice treated with vehicle. (**D**) Effect of acetate injection (i.p. 500 mg kg^{-1}) on food-intake in Wt mice. N = 8 mice, ****, $p < 0.0001$, Two-way ANOVA and Sidak's multiple comparisons tests. (**E**) Effect of acetate injection (i.p. 500 mg kg^{-1}) on food-intake in ob/ob mice. ****, $p < 0.0001$, two-way ANOVA and Sidak's multiple comparisons test. (**F**) Percent reduction of food-intake after acute acetate injection in Wt and ob/ob mice.*, $p < 0.05$, ****, $p < 0.0001$, two-way ANOVA and Sidak's multiple comparisons test. (**G**) NMR quantitative analysis of acetate concentration in the hypothalamus of obese and Wt mice in the vehicle and after 1 h, 2 h and 4 h post-injection. ***,### $p < 0.0001$, ##, $p < 0.01$ and *, $p < 0.05$, two-way ANOVA and Sidak's multiple comparisons test; ## = Wt, 1 h *vs* ob/ob, 1 h; # = Wt, 2 h *vs* ob/ob, 2 h.

immunohistochemical examination of the immunoreactivities of these two proteins in the hypothalamus of Wt and ob/ob mice, after vehicle or acetate injection. No colocalization was observed with GPR43 immunoreactivity in OX-A-immunoreactive cell bodies or processes, in both Wt and ob/ob mice (Fig. 2**C**) whereas expression of GPR43-immunoreactivity was mainly detected in the epithelia lining the 3rd ventricle, more intensely in ob/ob than in Wt mice (Fig.C) Acetate injection reduced both the intensity and the number of GPR43-positive cell profiles in both Wt and ob/ob mice (Fig. 2**C**).

Since the eCB 2-AG is both a potent modulator and a product of the activity of OX neurons [32,53], and SCFAs have been proposed to inhibit the expression of eCB biosynthetic enzymes [22], or of CB1 receptors [21], we quantified the levels of 2-AG in the hypothalamus of Wt, Wt + acetate, ob/ob and ob/ob + acetate treated mice by LC-APCI-MS. As expected, we observed an increase of 2-AG levels in ob/ob compared with Wt mice. Acetate treatment resulted in a reduction of 2-AG levels in ob/ob mice, whereas in Wt mice a trend towards an increase was observed (Fig. 2**D**).

3.3. Acetate reduces the firing of orexin neurons by increasing GABAergic transmission

To test if acetate directly modulates the firing rate of OX neurons, loose cell-attached recording was performed in *Hcrt*-eGFP neurons from lean mice. Acetate was tested at a concentration of 10.5 μM, corresponding to the maximal concentration of acetate found in the brain after an i.p. injection of 500 mg/kg [24]. Following a 10 min acetate treatment, a decrease in the firing rate was observed (Fig. 3**A, B**).

To better understand the mechanism by which acetate reduces the firing of OX neurons, the amplitude and frequency of sIPSCs were measured by patch clamp recordings on Hcrt-eGFP cells in Wt mice, in sections treated with acetate (10.5 μM) and acetate plus the GPR43 antagonist GLPG0974 (100 nM) [54]. In agreement with the decreased firing mentioned above, a significant increase in the frequency of sIPSCs was observed in acetate treated slices (Fig. 3**C, D**), whereas no differences were observed in the amplitude (Fig. 3**E**). This effect was prevented by GLPG0974.

Subsequently, we examined the effect of acetate on glutamatergic transmission at OX-A neurons. When comparing the frequency and

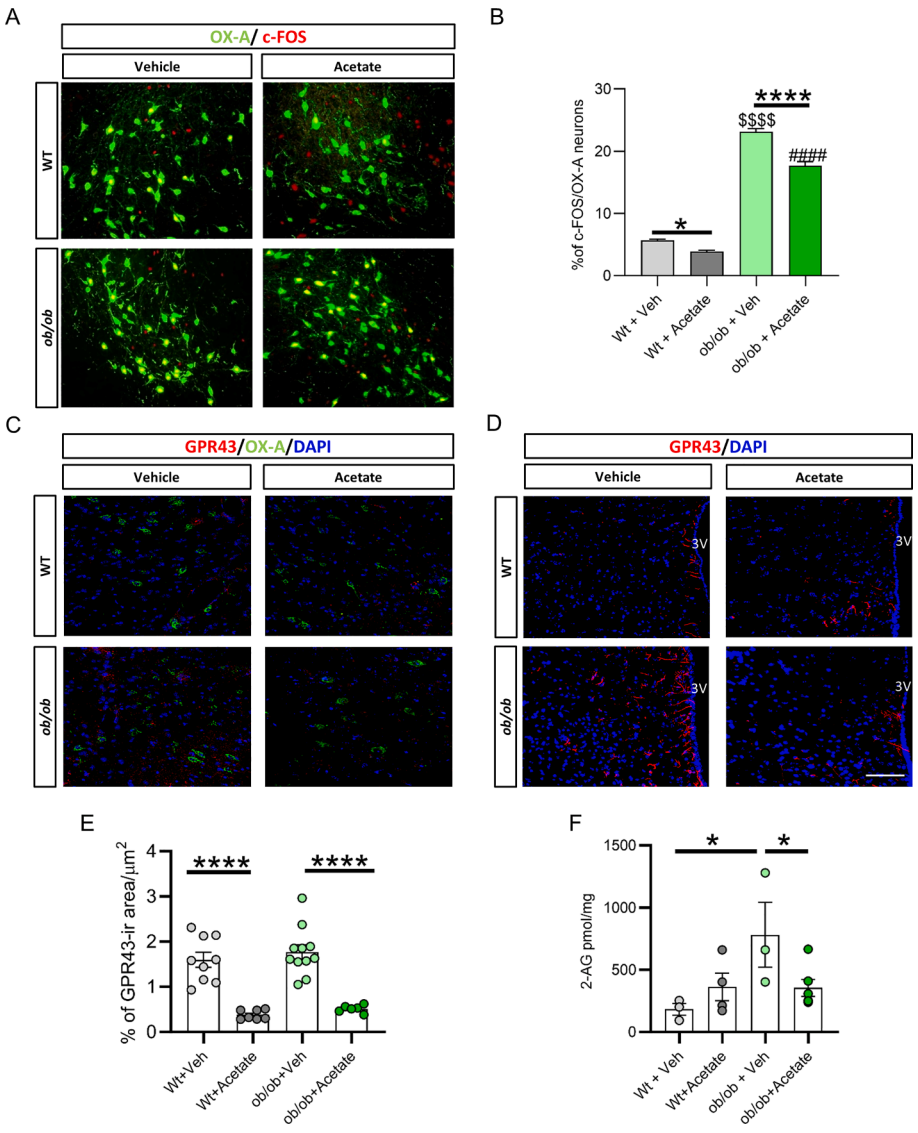

Fig. 2. Acetate modulates c-FOS expression in orexin neurons, GPR43 expression and eCB levels in obese mice. (**A**) c-FOS/OX-A double immunolabeling in the LH of Wt and ob/ob mice treated with vehicle or acetate. Hypothalamic leptin signal deficiency in ob/ob mice is accompanied by enhanced c-FOS expression in OX-A neurons. Acetate treatment (500 mg/kg i.p. for 1 h starting from ZT2) reduces c-FOS expression in OX-A neurons, both in Wt and ob/ob mice. Scale bar: 100 µm. (**B**) Bar graph showing the percentage of c-FOS/OX-A positive neurons in Wt and ob/ob mice after 1 h of injection with vehicle ($Wt_{veh} = 120 \pm 8$ cells) or acetate, calculated on the total of OX-A-positive neurons. Data are means ± SEM; n = 150 cells per group, n = 3 mice per group. *, $p < 0.05$, ****,####, $$$$, $p < 0.0001$, two-way ANOVA and Sidak's multiple comparisons test. * = Vehicle vs acetate, $ = Wt vehicle vs ob/ob vehicle, # = Wt acetate vs ob/ob acetate. (**C**) Representative coronal section of LH showing GPR43 and OX-A immunoexpression in Wt and ob/ob mice. No colocalization was observed in OX-A-immunoreactive cell bodies or dendritic spines with GPR43 immunoreactivity. (**D**) Representative coronal sections of the similar rostrocaudal position of the hypothalamic nuclei showing GPR43 labelled fibres and puncta in Wt and ob/ob mice. Elevated GPR43-immunoreactive expression occurs in untreated Wt and ob/ob mice. (**E**) Bar graph showing the percentage of GPR43 immunoreactivity/μm^2 from 100 μm^2 of an ROI area around the perifornical fornix as a reference point for vehicle- or acetate-injected Wt mice and vehicle- or acetate-treated ob/ob mice. ****, $p < 0.0001$, two-way ANOVA and Sidak's multiple comparisons test. (**F**) Bar graph of hypothalamic 2-AG levels in Wt + Veh, Wt + acetate, ob/ob + Veh and ob/ob + acetate mouse groups, *, $p < 0.05$, two-way ANOVA and Sidak's multiple comparisons test.

amplitude of sEPSCs no changes were observed in the control, acetate, and acetate + GLPG0974 groups (Fig. 3**F, G, H**).

3.4. Acetate increases depolarization-induced suppression of excitation onto orexinergic neurons

Because acetate showed the ability to modulate hypothalamic 2-AG levels, the eCB-mediated DSE of sEPSCs was examined in Hcrt-eGFP neurons from lean mice. A baseline of sEPSCs (Vc: −60 mV) was recorded for 15 sec, then a 5 sec depolarization step was applied at 0 mV, and finally, the sEPSC frequency was measured for 20 sec at −60 mV (Fig. 4**A**). We report the percent changes in frequency and amplitude from baseline, calculated in the 5-sec bin before and after the depolarization step. Analysis of DSE in OX neurons showed that the sEPSC frequency variation in comparison to the baseline had the same trend in the three groups (Fig. 4**B**), whereas the decrease of sEPSC amplitude lasted longer in the acetate- and acetate + GLPG0974-treated slices (Fig. 4**C**). The induction of 2-AG production and release by our protocol of DSE was confirmed by using the CB1R antagonist AM251, which completely abolished the reduction in frequency of sIPSCs observed after the depolarizing step (Fig. 4**D**).

On the other hand, the data obtained from the DSI analysis was controversial since we observed a significant decrease in the frequency of sIPSCs, which lasted 15-sec in control and 20-sec in acetate and

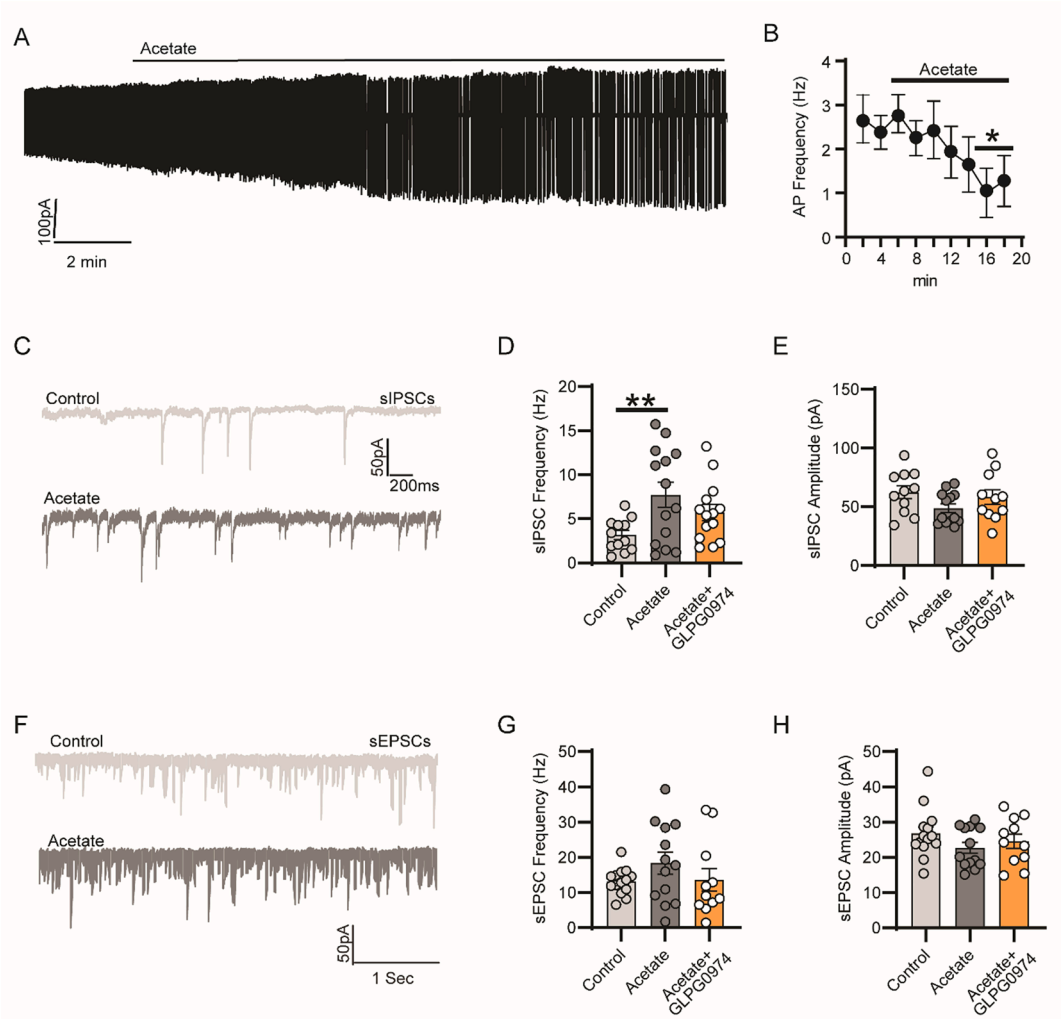

Fig. 3. Acetate decreases the activity of orexin neurons by enhancing GABAergic transmission. (**A**) Representative trace and scheme of cell-attached recording in Hcrt-eGFP neurons in the control condition and during the application of acetate 10.5 μM. (**B**). Time course of Hcrt-eGFP neuron action potential frequency before and during acetate treatment. *, $p < 0.05$, two-tailed paired Wilcoxon's signed-rank test. n = 9 from 4 mice. Two-tailed paired Wilcoxon's signed-rank test. (**C**) Representative traces of sIPSCs were recorded in Hcrt-eGFP lean mouse slices in control and acetate (10.5 μM) groups. (**D**) Bar graph of sIPSC frequency recorded in untreated, acetate and acetate + GLPG0974 (100 nM), **, $p < 0.01$, Brown-Forsythe and Welch ANOVA test, 3 mice per group. (**E**) Bar graph of sIPSC amplitude recorded in control, acetate and acetate + GLPG0974. (**F**) Representative traces of sEPSCs recorded in Hcrt-eGFP lean mouse slices in control and acetate 10.5 μM groups. (**G**) Bar graph of sEPSC frequency recorded in control, acetate and acetate + GLPG0974 groups (100 nM). (**H**) Bar graph of sEPSC amplitude recorded in control, acetate and acetate + GLPG0974 groups.

acetate + GLPG0974 (Fig. 5**A, B**). Conversely, the amplitude of sIPSC was enhanced after the 5-sec depolarization step in both acetate and acetate + GLPG0974 groups vs the control group (Fig. 5**C**). Finally, we tested if the CB1R inhibition was sufficient to block the ability of acetate to reduce the firing rate of OX-A neurons. We still detect a reduction of the firing rate after acetate treatment in the hypothalamic slice of Hcrt-eGFP mice pretreated with CB1R antagonist AM251 (4 μM) (Fig. 5**D, E, F**).

A parsimonious interpretation of these data, and those reported in the previous section, is that acetate reduces orexin neuron firing in lean mice via a mechanism that is mostly GPR43-dependent and CB1-independent.

3.5. Acetate and orexin modulate POMC mRNA levels in opposing manners

It has been suggested that the anorectic effects of acetate administration are mediated by a change in hypothalamic neuropeptides and in particular by an increase in POMC and a decrease in NPY and AgRP via an increase in malonyl-CoA concentrations [24]. However, POMC neurons are also inhibited by OX neurons [55]. We observed here that injection of OX in mice negatively modulated *Pomc* mRNA levels, this effect being counteracted by SB334867, an orexin-1 receptor inhibitor (Fig. 6). Injection of acetate instead enhanced POMC mRNA levels, in agreement with Frost et al. [24], and co-injection with OX could only reduce the extent of this effect, possibly due to additive opposing effects (Fig. 6). These data, together with those described in the previous sections, suggest that acetate might enhance POMC neurons also by inhibiting OX signaling.

4. Discussion

SCFAs have demonstrated diverse effects, including anti-inflammatory, anti-obesity, and neuroprotective properties [56], but their precise mechanism of action at the cerebral level remains poorly understood. The present study was based on prior observations indicating that acetate diminishes food-intake and increases POMC-derived peptide release [24]. Our investigation focused on the effects of acetate supplementation on OX-A neurons, a cluster of cells situated in the LH crucial for energy homeostasis. Through a multidisciplinary approach,

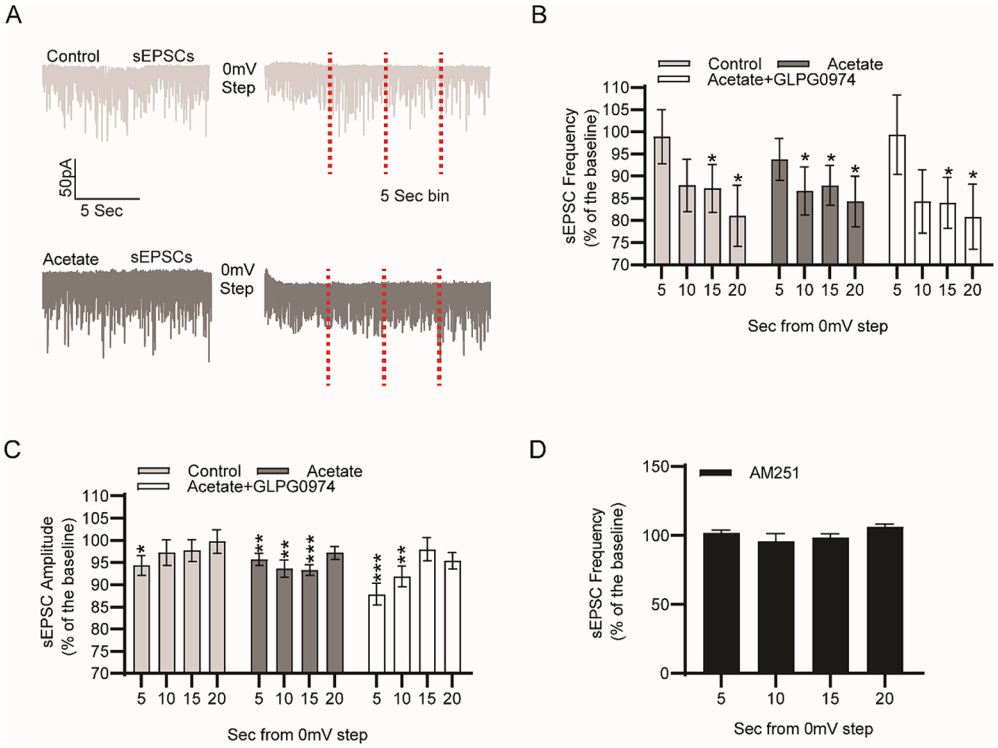

Fig. 4. Acetate enhances DSE onto OX-A neurons. (**A**) Representative traces of the sEPSC-DSE in untreated and acetate 10.5 μM treated slices. After 10 sec of baseline at −60 mV, Hcrt-eGFP neurons were depolarized for 5 sec at 0 mV and then clamped at −60 mV for 20 sec. Vertical red lines indicate the 5 sec bins. (**B**) Percentage changes of sEPSC frequency relative to 100 % baseline in the control (12,8 ± 1,12 Hz at t_{5sec}), acetate (16,66 ± 2,6Hz at t_{5sec}) and acetate + GLPG0974 (13,35 ± 2,9Hz at t_{5sec}) groups. The comparison of each group at a given time point compared to a 100 % baseline was performed using one sample *t*-test. (**C**) Percentage changes of sEPSC amplitude relative to 100 % baseline in the control (25,33 ± 1,7pA at t_{5sec}), acetate (21,68 ± 1,4pA at t_{5sec}) and acetate + GLPG0974 (21,27 ± 1,5pA at t_{5sec}) groups. The comparison of each group at a given time point compared to the baseline was performed using a one-sample *t*-test, and the intergroup analysis was performed using two-way ANOVA and Sidak's multiple comparisons test. *, $p < 0.05$, **, $p < 0.01$, ***, $p < 0.001$. (**D**) Percentage changes of sEPSC frequency relative to 100 % baseline (14,10 ± 2,1Hz) in slices preincubated with AM251 (4 μM).

our findings suggest that the anorexigenic impact of acetate is partially attributable to the reduction of OX-A neuronal activity in both Wt and ob/ob mice.

Obesity induces alterations in acetate metabolism. Despite prior reports indicating increased (or unchanged) concentrations of intestinal acetate in obese mice [13,27], our study reveals a diminished concentration of this molecule in the hypothalamus of obese mice. These data are consistent with an increase in acetate metabolism in adipose tissue in obesity [49,50]. Notably, while acetate injection induces an anorectic effect within the initial hour in both Wt and ob/ob mice, this effect diminishes in obese mice, likely due to accelerated acetate metabolism by adipose tissue [49,50]. Accordingly, while we observed an increment in the acetate concentration in the brain of Wt mice at 1 h and 2 h post-injection we failed to observe any variation of acetate concentration in the brains of ob/ob mice.

A limitation of our study arises from the fact that the protocol for measuring food-intake does not adhere to the circadian rhythm of mice. However, we opted for this approach in line with the literature [24]. Animals were subjected to caloric restriction for 12 h before testing, to enhance their motivation to eat during the test despite they are in resting phase. Nonetheless, the data obtained remain consistent with existing literature on the effects of acetate on food-intake and with published findings implicating orexin neurons in the regulation of the dopaminergic system and motivation in both lean [57,58] and in ob/ob mice [59].

Furthermore, we report here the influence of acetate on the orexinergic system, presenting a novel mechanism for the regulation of food-intake. Our findings support the notion that acetate reduces appetite by entering in the glutamate–glutamine cycle and supporting GABAergic neurotransmission directly onto OX neurons [24,60]. Our electrophysiological recordings in hypothalamic brain slices from Hcrt-eGFP mice demonstrate that acetate treatment triggers an increase in sIPSC frequency via the GPR43 receptor without affecting glutamatergic neurotransmission. This effect is mediated by the network surrounding the OX cell since no co-immunolocalization was found between orexin neurons and the GPR43 receptor. On the other hand, GPR43 does not seem to be expressed in astrocytes, the other source of glutamine fundamental in the GABA synthesis [61]. Moreover, we have shown that chronic injection of acetate modulates the levels of GPR43 in the brain, which is indicative of receptor activation followed by desensitization. The expression of GPR43 and its precise role in enhancing GABA transmission remain to be fully determined.

We cannot exclude the possibility that acetate modulates neuronal activity of OX-A neurons via other mechanisms, such as by modulating K^+ conductance, as has been observed in the colon [62,63]. Notably, the increase in POMC reported in the presence of acetate may contribute to the decreased activity of OX neurons itself. Indeed, POMC neurons are known to electrically inhibit OX cells [55]. Conversely, acetate may owe part of its effect on POMC to its inhibition of OX signalling, since in an experiment with double injection of acetate and orexin into lean mice, we observed an increase in POMC mRNA, a sign that acetate can counteract orexin signalling, which alone causes POMC mRNA depletion (see also [33]). Finally, activation of vagal afferents and an increase in leptin levels have been reported to play a role in the acetate-mediated reduction in food-intake [64–66].

It has been proposed that acetate modulates the eCB system [22]. We observed a decline in 2-AG levels following acetate treatments in ob/ob mice, possibly attributable to elevated baseline 2-AG levels in obese mice compared to Wt, an effect that we previously showed to be due in part to higher orexin activity [33]. Our electrophysiological recordings

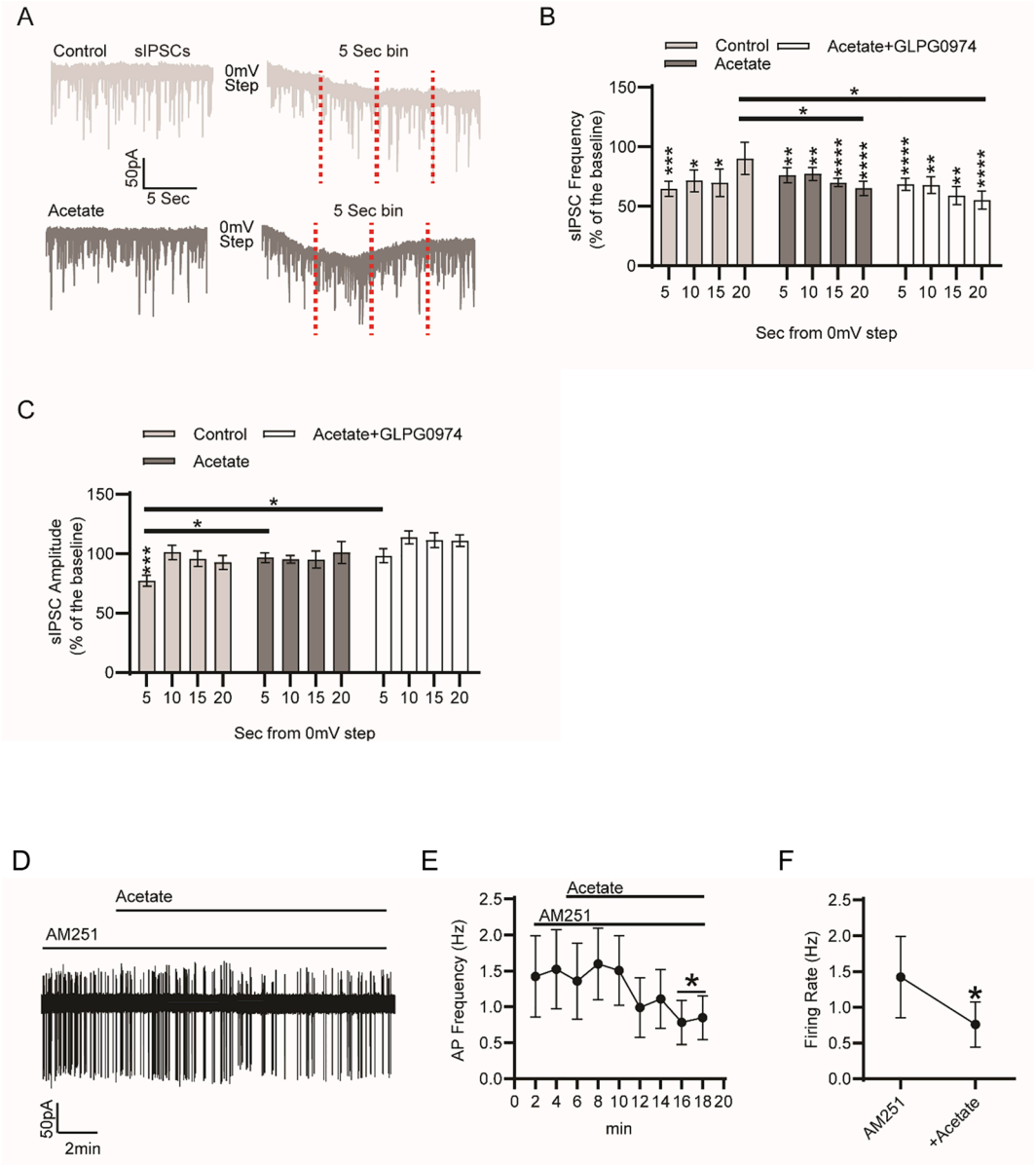

Fig. 5. Acetate modulates DSI onto OX-A neurons. (A) Representative traces of the sIPSC-DSI in control and acetate. After 10 sec of baseline at −60 mV, Hcrt-eGFP neurons were depolarized for 5 s at 0 mV and then clamped at −60 mV for 20 s. Vertical red lines indicate the 5-s bins. (**B**) Percentage changes of sIPSC frequency relative to 100 % baseline in the control (1,85 ± 0,2Hz at t_{5sec}), acetate (6,1 ± 1,1Hz at t_{5sec}) and acetate + GLPG0974 (3,9 ± 0,6Hz at t_{5sec}) groups. The comparison of each group at a given time point compared to 100 % baseline was performed using One sample *t*-test, and the intergroup analysis was performed using Two-way ANOVA and Sidak's multiple comparisons test. (**C**) Percentage changes of sIPSC amplitude relative to 100 % baseline in the control (52,69 ± 7,2pA at t_{5sec}), acetate (53,22 ± 8,1pA at t_{5sec}) and acetate + GLPG0974 (52,13 ± 6,4pA at t_{5sec}) groups. The comparison of each group at a given time point compared to the baseline was performed using a one-sample *t*-test, and the intergroup analysis was performed using two-way ANOVA and Sidak's multiple comparisons test. *, $p < 0.05$, **, $p < 0.01$, ***, $p < 0.001$, ****, $p < 0.0001$. (**D**) Representative trace of cell-attached recording in *Hcrt*-eGFP neurons in the presence of AM251 before and after acetate 10.5 μM. (**E**) Time course of Hcrt-eGFP neuron action potential frequency before and during acetate treatment. *, $p < 0.05$, two-tailed paired Wilcoxon's signed-rank test. (**F**). Mean ± SEM of the AP frequency of Hcrt-eGFP neurons in AM251 and after acetate treatment. n = 6 from 4 mice. *, $p < 0.05$, two-tailed paired Wilcoxon's signed-rank test.

of DSE/DSI suggest a cell-specific role for acetate in the two forms of synaptic plasticity in hypothalamic slices of Hcrt-eGFP Wt mice, previously (and here) shown to be 2-AG/CB1-mediated [32]. However, the eCB system does not appear to be the primary mechanism by which acetate diminishes the firing of OX neurons in lean mice, as CB1 receptor antagonism with AM251 did not prevent the reduction in firing rate of Hcrt-eGFP neurons in the presence of acetate, an effect that was, instead, fully prevented by a GPR43 antagonist. Therefore, we propose that acetate reduces orexin neuron firing in lean mice via a mechanism that is mostly GPR43-dependent and CB1-independent. Nevertheless, CB1-dependent DSE might also play a (not necessary) role, since its duration, in terms of reduction of sEPSC amplitude, was enhanced by acetate (in a GPR43-independent manner), in agreement with the non-statistically significant elevation by this SCFA of 2-AG levels observed in hypothalamic slices from Wt mice. However, the fact that acetate significantly reduced 2-AG levels in hypothalamus from ob/ob mice suggests that, if anything, in these mice, we might have found a weaker DSE with the SCFA, which would have been inconsistent with – and/or insufficient to reverse – the observed decrease of orexin neuron activity. This hypothesis is also supported by the previously observed decrease of excitatory/glutamatergic terminals onto orexinergic neurons of ob/ob mice [32]. Regarding DSI, this form of plasticity is, instead, unlikely to

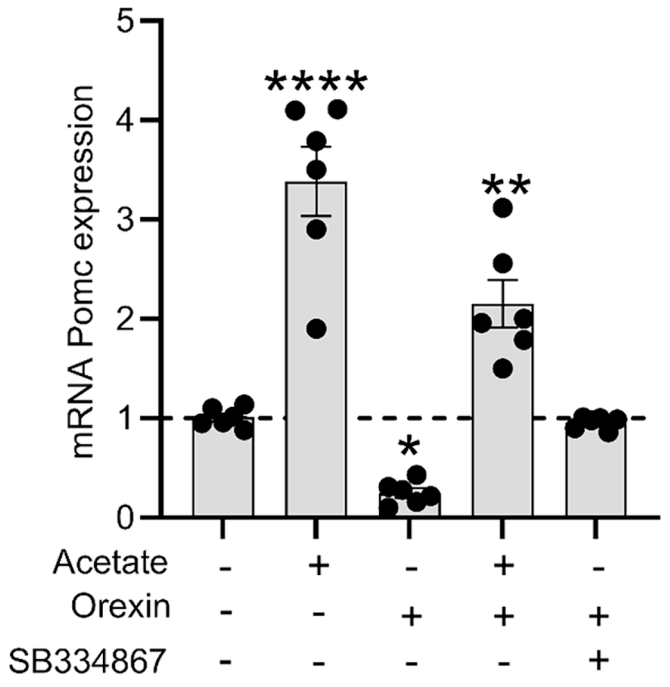

Fig. 6. Acetate and orexin modulate POMC mRNA levels. Reduced Pomc mRNA expression in the mouse arcuate nucleus (ARC) is triggered by i.p. injection of OX-A and prevented by co-treatment with SB3334867, while acetate enhances *Pomc* mRNA expression. The bar graph of the mRNA levels is reported as normalized to the reference genes *Hprt* and *β-actin* and each condition was scaled to the control value (no-treated mice) as baseline (dotted line). The mean of the quantitative cycles (Cq) for the Control was 22.41 (SD = 0.054). The Cq of the negative controls (NTC) were undetectable for up to 40 reaction cycles. ANOVA with Bonferroni post hoc test, *, $p < 0.05$, **, $p < 0.01$, ****, $p < 0.0001$. Expression differences between Control vs OX-A, OX-A vs OX-A + SB334867 were significant as evaluated by the REST® software [77] (*, $p < 0.05$).

participate in acetate-induced inhibition of orexin neuron firing in lean since the data on sIPSC frequency indicate an increase in DSI, while the data on sIPSC amplitude suggest a decrease of DSI under acetate treatment. However, we speculate that in ob/ob mice, where acetate reduced hypothalamic 2-AG levels, DSI would have been reduced, in agreement with the observed decrease of orexin neuron activity. Indeed, acetate may produce its inhibitory effect on orexinergic activity in ob/ob mice through reduced DSI, since: 1) this form of synaptic plasticity was shown to prevail on DSE and underlie, instead, increased basal orexinergic neuron activity in these as well as in diet-induced obese (DIO) mice [32], and 2) stimulation of GABAergic transmission onto these same neurons were shown here to underlie the effects of acetate in lean mice. It will be, therefore, of great importance to study the effect of acetate on orexinergic cells, and on the surrounding neural network, in obese mice in correlation with the eCB system using *Hcrt*-eGFP DIO mice.

OX-A signalling is enhanced in obesity [32,67], and alterations of OX/eCBs levels have been linked to alteration of memory performance [67]. It is intriguing to speculate that acetate, which reduces OX discharge, could theoretically enhance cognitive performance in obesity [67]. Indeed, dietary fibre deficiency has been demonstrated to alter SCFA levels and impair memory in mice [68]. Thus, the interaction between SCFAs and OX-A neurons might play a crucial role also in connecting gut dysbiosis to cognitive decline in obesity.

Interventions targeting the gut microbiota, such as dietary modifications and probiotic supplements, are areas of ongoing research for potential therapeutic strategies in the management of obesity and related metabolic disorders [69]. A high-fiber diet can mitigate weight gain by regulating food-intake and appetite while fostering the growth and activity of bacteria that produce SCFAs [70]. Specifically, bacteria belonging to the genera *Coprococcus, Barnesiella*, *Ruminococcus*, and *Ruminococcaceae* NK4A21 demonstrated a positive correlation with circulating acetate levels, while *Lachnoclostridium* and *Bacteroides* exhibited a negative correlation [70]. It is well-established that SCFA-producing bacteria like *Akkermansia* and *Bifidobacterium*, essential components of a healthy gut microbiota, are diminished in obesity [71,72]. Studies have shown that modifying the gut microbiome in ob/ob mice by selectively increasing *Bifidobacterium* improves gut permeability and reduces inflammation, both attributed to the actions of acetate on inflammation [73,74]. On the other hand, the supplementation with a probiotic containing *Lactobacillus rhamnosus*, *Lactobacillus acidophilus*, and *Bifidobacterium bifidum,* in line with an increment in acetate levels, reduced body weight and food-intake in diet-induced obese mice [75,76].

In conclusion, based on data presented here and previously published, our study supports the concept that acetate and the probiotic supplementation of acetate-producing bacteria may represent novel anti-obesity strategies, and enlarges our perspectives on the mechanism of action of this SCFA.

Funding

EU financial support PON IDF SHARID code ARS01_01270, to L.C. and V.D. CNR project FOE-2021 "NutrAge" – code DBA.AD005.225 to L.C.; PRIN- PNRR code NASC20222 “NeuroFood” to L.C. M.P.M. and V.D.; Joint International Research Unit (JIRU) for Chemical and Biomolecular Research on the Microbiome and its impact on Metabolic Health and Nutrition (MicroMeNu) and the Sentinelle Nord Program of Université Laval to L.C., and V.D., which in turn are funded by the Canada First/Apogée program of the Tri-Agency of the Canadian Federal Government. EU PNRR grant code "OnFood" n.PE10 to B.M and M.P.M.

CRediT authorship contribution statement

Nicola Forte: Writing – original draft, Validation, Methodology, Formal analysis. **Brenda Marfella:** Methodology. **Alessandro Nicois:** Methodology. **Letizia Palomba:** Validation, Methodology, Conceptualization. **Debora Paris:** Methodology, Formal analysis. **Andrea Motta:** Validation, Resources. **Maria Pina Mollica:** Funding acquisition, Conceptualization. **Vincenzo Di Marzo:** Writing – review & editing, Funding acquisition, Conceptualization. **Luigia Cristino:** Writing – review & editing, Writing – original draft, Resources, Project administration, Funding acquisition, Data curation, Conceptualization.

Declaration of competing interest

The authors declare that they have no known competing financial interests or personal relationships that could have appeared to influence the work reported in this paper.

Data availability

Data will be made available on request.

Acknowledgements

Dr Roberta Verde and Dr Fabiana Piscitelli for conducting biochemical measurements using LC-MS mass spectrometry; Dr Nadia Cacciapuoti and Dr. Lea Tunisi for providing technical support for the immunohistochemical study.

References

[1] A. Moura-Assis, J.M. Friedman, L.A. Velloso, Gut-to-brain signals in feeding control, Am. J. Physiol.-Endocrinol. Metab. 320 (2021) E326–E332, https://doi.org/10.1152/ajpendo.00388.2020.

[2] M. Carabotti, A. Scirocco, M.A. Maselli, C. Severi, The gut-brain axis: interactions between enteric microbiota, central and enteric nervous systems, Ann. Gastroenterol. 28 (2015) 203–209.

[3] B.O. Schroeder, F. Backhed, Signals from the gut microbiota to distant organs in physiology and disease, Nat. Med. 22 (2016) 1079–1089, https://doi.org/10.1038/nm.4185.

[4] H.-D. Mir, G. Giorgini, V. Di Marzo, The emerging role of the endocannabinoidome-gut microbiome axis in eating disorders, Psychoneuroendocrinology 154 (2023) 106295, https://doi.org/10.1016/j.psyneuen.2023.106295.

[5] J. van Son, L.L. Koekkoek, S.E. La Fleur, M.J. Serlie, M. Nieuwdorp, The Role of the Gut Microbiota in the Gut-Brain Axis in Obesity: Mechanisms and Future Implications, IJMS 22 (2021) 2993, https://doi.org/10.3390/ijms22062993.

[6] T.V. Rohm, D.T. Meier, J.M. Olefsky, M.Y. Donath, Inflammation in obesity, diabetes, and related disorders, Immunity 55 (2022) 31–55, https://doi.org/10.1016/j.immuni.2021.12.013.

[7] C.L. Roth, H. Eslamy, D. Werny, C. Elfers, M.L. Shaffer, C. Pihoker, J. Ojemann, W. B. Dobyns, Semiquantitative analysis of hypothalamic damage on MRI predicts risk for hypothalamic obesity, Obesity 23 (2015) 1226–1233, https://doi.org/10.1002/oby.21067.

[8] R.E. Ley, P.J. Turnbaugh, S. Klein, J.I. Gordon, Microbial ecology: human gut microbes associated with obesity, Nature 444 (2006) 1022–1023, https://doi.org/10.1038/4441022a.

[9] R.E. Ley, F. Bäckhed, P. Turnbaugh, C.A. Lozupone, R.D. Knight, J.I. Gordon, Obesity alters gut microbial ecology, Proc. Natl. Acad. Sci. u.s.a. 102 (2005) 11070–11075, https://doi.org/10.1073/pnas.0504978102.

[10] T.C. Fung, The microbiota-immune axis as a central mediator of gut-brain communication, Neurobiol. Dis. 136 (2020) 104714, https://doi.org/10.1016/j.nbd.2019.104714.

[11] H. Han, B. Yi, R. Zhong, M. Wang, S. Zhang, J. Ma, Y. Yin, J. Yin, L. Chen, H. Zhang, From gut microbiota to host appetite: gut microbiota-derived metabolites as key regulators, Microbiome 9 (2021) 162, https://doi.org/10.1186/s40168-021-01093-y.

[12] J. Breton, M. Galmiche, P. Déchelotte, Dysbiotic Gut Bacteria in Obesity: An Overview of the Metabolic Mechanisms and Therapeutic Perspectives of Next-Generation Probiotics, Microorganisms 10 (2022) 452, https://doi.org/10.3390/microorganisms10020452.

[13] P.J. Turnbaugh, R.E. Ley, M.A. Mahowald, V. Magrini, E.R. Mardis, J.I. Gordon, An obesity-associated gut microbiome with increased capacity for energy harvest, Nature 444 (2006) 1027–1031, https://doi.org/10.1038/nature05414.

[14] M. van de Wouw, H. Schellekens, T.G. Dinan, J.F. Cryan, Microbiota-Gut-Brain Axis: Modulator of Host Metabolism and Appetite, J. Nutr. 147 (2017) 727–745, https://doi.org/10.3945/jn.116.240481.

[15] M.-A. Levrat, C. Rémésy, C. Demigné, High Propionic Acid Fermentations and Mineral Accumulation in the Cecum of Rats Adapted to Different Levels of Inulin, J. Nutr. 121 (1991) 1730–1737, https://doi.org/10.1093/jn/121.11.1730.

[16] K. Nishitsuji, J. Xiao, R. Nagatomo, H. Umemoto, Y. Morimoto, H. Akatsu, K. Inoue, K. Tsuneyama, Analysis of the gut microbiome and plasma short-chain fatty acid profiles in a spontaneous mouse model of metabolic syndrome, Sci Rep 7 (2017) 15876, https://doi.org/10.1038/s41598-017-16189-5.

[17] T. Ilyés, C.N. Silaghi, A.M. Crăciun, Diet-Related Changes of Short-Chain Fatty Acids in Blood and Feces in Obesity and Metabolic Syndrome, Biology 11 (2022) 1556, https://doi.org/10.3390/biology11111556.

[18] C. Manca, B. Boubertakh, N. Leblanc, T. Deschenes, S. Lacroix, C. Martin, A. Houde, A. Veilleux, N. Flamand, G.G. Muccioli, F. Raymond, P.D. Cani, V. Di Marzo, C. Silvestri, Germ-free mice exhibit profound gut microbiota-dependent alterations of intestinal endocannabinoidome signaling, J. Lipid Res. 61 (2020) 70–85, https://doi.org/10.1194/jlr.RA119000424.

[19] C. Manca, M. Shen, B. Boubertakh, C. Martin, N. Flamand, C. Silvestri, V., Di Marzo, Alterations of brain endocannabinoidome signaling in germ-free mice, Biochimica et Biophysica Acta (BBA), in: Molecular and Cell Biology of Lipids 1865, 2020, p. 158786, https://doi.org/10.1016/j.bbalip.2020.158786.

[20] A. Vijay, A. Kouraki, S. Gohir, J. Turnbull, A. Kelly, V. Chapman, D.A. Barrett, W. J. Bulsiewicz, A.M. Valdes, The anti-inflammatory effect of bacterial short chain fatty acids is partially mediated by endocannabinoids, Gut Microbes 13 (2021) 1997559, https://doi.org/10.1080/19490976.2021.1997559.

[21] H. Kalkan, E. Pagano, D. Paris, E. Panza, M. Cuozzo, C. Moriello, F. Piscitelli, A. Abolghasemi, E. Gazzerro, C. Silvestri, R. Capasso, A. Motta, R. Russo, V. Di Marzo, F.A. Iannotti, Targeting gut dysbiosis against inflammation and impaired autophagy in Duchenne muscular dystrophy, EMBO Mol Med 15 (2023) e16225. https://doi.org/10.15252/emmm.202216225.

[22] I.Y. Hwang, H.R. Kim, R. De Sotto, M.W. Chang, Engineered probiotics modulate the endocannabinoid system, Biotechnology Notes 2 (2021) 33–38, https://doi.org/10.1016/j.biotno.2021.08.001.

[23] K.N. Kim, Y. Yao, S.Y. Ju, Short Chain Fatty Acids and Fecal Microbiota Abundance in Humans with Obesity: A Systematic Review and Meta-Analysis, Nutrients 11 (2019) 2512, https://doi.org/10.3390/nu11102512.

[24] G. Frost, M.L. Sleeth, M. Sahuri-Arisoylu, B. Lizarbe, S. Cerdan, L. Brody, J. Anastasovska, S. Ghourab, M. Hankir, S. Zhang, D. Carling, J.R. Swann, G. Gibson, A. Viardot, D. Morrison, E. Louise Thomas, J.D. Bell, The short-chain fatty acid acetate reduces appetite via a central homeostatic mechanism, Nature Communications 5 (2014) 3611, https://doi.org/10.1038/ncomms4611.

[25] K.S. Olaniyi, M.N. Owolabi, C.L. Atuma, T.B. Agunbiade, B.Y. Alabi, Acetate rescues defective brain-adipose metabolic network in obese Wistar rats by modulation of peroxisome proliferator-activated receptor-γ, Sci Rep 11 (2021) 18967, https://doi.org/10.1038/s41598-021-98605-5.

[26] R.J. Perry, L. Peng, N.A. Barry, G.W. Cline, D. Zhang, R.L. Cardone, K.F. Petersen, R.G. Kibbey, A.L. Goodman, G.I. Shulman, Acetate mediates a microbiome-brain-β-cell axis to promote metabolic syndrome, Nature 534 (2016) 213–217, https://doi.org/10.1038/nature18309.

[27] F. Suriano, S. Vieira-Silva, G. Falony, M. Roumain, A. Paquot, R. Pelicaen, M. Régnier, N.M. Delzenne, J. Raes, G.G. Muccioli, M. Van Hul, P.D. Cani, Novel insights into the genetically obese (ob/ob) and diabetic (db/db) mice: two sides of the same coin, Microbiome 9 (2021) 147, https://doi.org/10.1186/s40168-021-01097-8.

[28] I. Gabanyi, G. Lepousez, R. Wheeler, A. Vieites-Prado, A. Nissant, S. Wagner, C. Moigneu, S. Dulauroy, S. Hicham, B. Polomack, F. Verny, P. Rosenstiel, N. Renier, I.G. Boneca, G. Eberl, P.-M. Lledo, Bacterial sensing via neuronal Nod2 regulates appetite and body temperature, Science 376 (2022) eabj3986, https://doi.org/10.1126/science.abj3986.

[29] I. Villano, M. La Marra, G. Di Maio, V. Monda, S. Chieffi, E. Guatteo, G. Messina, F. Moscatelli, M. Monda, A. Messina, Physiological Role of Orexinergic System for Health, IJERPH 19 (2022) 8353, https://doi.org/10.3390/ijerph19148353.

[30] T. Sakurai, A. Amemiya, M. Ishii, I. Matsuzaki, R.M. Chemelli, H. Tanaka, S. C. Williams, J.A. Richardson, G.P. Kozlowski, S. Wilson, J.R. Arch, R. E. Buckingham, A.C. Haynes, S.A. Carr, R.S. Annan, D.E. McNulty, W.S. Liu, J. A. Terrett, N.A. Elshourbagy, D.J. Bergsma, M. Yanagisawa, Orexins and orexin receptors: a family of hypothalamic neuropeptides and G protein-coupled receptors that regulate feeding behavior, Cell 92 (1998) 573–585, https://doi.org/10.1016/s0092-8674(00)80949-6.

[31] Y. Yoshida, N. Fujiki, T. Nakajima, B. Ripley, H. Matsumura, H. Yoneda, E. Mignot, S. Nishino, Fluctuation of extracellular hypocretin-1 (orexin A) levels in the rat in relation to the light-dark cycle and sleep-wake activities, Eur. J. Neurosci. 14 (2001) 1075–1081, https://doi.org/10.1046/j.0953-816x.2001.01725.x.

[32] L. Cristino, G. Busetto, R. Imperatore, I. Ferrandino, L. Palomba, C. Silvestri, S. Petrosino, P. Orlando, M. Bentivoglio, K. Mackie, V. Di Marzo, Obesity-driven synaptic remodeling affects endocannabinoid control of orexinergic neurons., Proceedings of the National Academy of Sciences of the United States of America 110 (2013) E2229-38. https://doi.org/10.1073/pnas.1219485110.

[33] G. Morello, R. Imperatore, L. Palomba, C. Finelli, G. Labruna, F. Pasanisi, L. Sacchetti, L. Buono, F. Piscitelli, P. Orlando, V. Di Marzo, L. Cristino, Orexin-A represses satiety-inducing POMC neurons and contributes to obesity via stimulation of endocannabinoid signaling., Proceedings of the National Academy of Sciences of the United States of America 113 (2016) 4759–4764. https://doi.org/10.1073/pnas.1521304113.

[34] F. Berrendero, Á. Flores, P. Robledo, When orexins meet cannabinoids: Bidirectional functional interactions, Biochem. Pharmacol. 157 (2018) 43–50, https://doi.org/10.1016/j.bcp.2018.08.040.

[35] M. Kano, T. Ohno-Shosaku, Y. Hashimotodani, M. Uchigashima, M. Watanabe, Endocannabinoid-Mediated Control of Synaptic Transmission, Physiol. Rev. 89 (2009) 309–380, https://doi.org/10.1152/physrev.00019.2008.

[36] A.C. Kreitzer, W.G. Regehr, Retrograde Inhibition of Presynaptic Calcium Influx by Endogenous Cannabinoids at Excitatory Synapses onto Purkinje Cells, Neuron 29 (2001) 717–727, https://doi.org/10.1016/S0896-6273(01)00246-X.

[37] M. Isokawa, B.E. Alger, Retrograde endocannabinoid regulation of GABAergic inhibition in the rat dentate gyrus granule cell: Endogenous cannabinoid transmission in the dentate gyrus, J. Physiol. 567 (2005) 1001–1010, https://doi.org/10.1113/jphysiol.2005.094219.

[38] H. Huang, C. Acuna-Goycolea, Y. Li, H.M. Cheng, K. Obrietan, A.N. van den Pol, Cannabinoids excite hypothalamic melanin-concentrating hormone but inhibit hypocretin/orexin neurons: implications for cannabinoid actions on food-intake and cognitive arousal, J. Neurosci. 27 (2007) 4870–4881, https://doi.org/10.1523/JNEUROSCI.0732-07.2007.

[39] P. Marcos, R. Coveñas, Involvement of the Orexinergic System in Feeding, Appl. Sci. 12 (2021) 86, https://doi.org/10.3390/app12010086.

[40] C. Mediavilla, Bidirectional gut-brain communication: A role for orexin-A, Neurochem. Int. 141 (2020) 104882, https://doi.org/10.1016/j.neuint.2020.104882.

[41] D. Paris, D. Melck, M. Stocchero, O. D'Apolito, R. Calemma, G. Castello, F. Izzo, G. Palmieri, G. Corso, A. Motta, Monitoring liver alterations during hepatic tumorigenesis by NMR profiling and pattern recognition, Metabolomics 6 (2010) 405–416, https://doi.org/10.1007/s11306-010-0209-8.

[42] T.L. Hwang, A.J. Shaka, Water Suppression That Works. Excitation Sculpting Using Arbitrary Wave-Forms and Pulsed-Field Gradients, Journal of Magnetic Resonance, Series A 112 (1995) 275–279. https://doi.org/10.1006/jmra.1995.1047.

[43] T.-W.-M. Fan, Metabolite profiling by one- and two-dimensional NMR analysis of complex mixtures, Prog. Nucl. Magn. Reson. Spectrosc. 28 (1996) 161–219, https://doi.org/10.1016/0079-6565(95)01017-3.

[44] D.S. Wishart, A. Guo, E. Oler, F. Wang, A. Anjum, H. Peters, R. Dizon, Z. Sayeeda, S. Tian, B.L. Lee, M. Berjanskii, R. Mah, M. Yamamoto, J. Jovel, C. Torres-Calzada, M. Hiebert-Giesbrecht, V.W. Lui, D. Varshavi, D. Varshavi, D. Allen, D. Arndt, N. Khetarpal, A. Sivakumaran, K. Harford, S. Sanford, K. Yee, X. Cao, Z. Budinski, J. Liigand, L. Zhang, J. Zheng, R. Mandal, N. Karu, M. Dambrova, H.B. Schiöth, R. Greiner, V. Gautam, HMDB 5.0: the Human Metabolome Database for 2022, Nucleic Acids Res. 50 (2022) D622–D631, https://doi.org/10.1093/nar/gkab1062.

[45] G.A. Bewick, A. Kent, D. Campbell, M. Patterson, M.A. Ghatei, S.R. Bloom, J. V. Gardiner, Mice With Hyperghrelinemia Are Hyperphagic and Glucose Intolerant and Have Reduced Leptin Sensitivity, Diabetes 58 (2009) 840–846, https://doi.org/10.2337/db08-1428.

[46] F. Piscitelli, G. Carta, T. Bisogno, E. Murru, L. Cordeddu, K. Berge, S. Tandy, J. S. Cohn, M. Griinari, S. Banni, V. Di Marzo, Effect of dietary krill oil

supplementation on the endocannabinoidome of metabolically relevant tissues from high-fat-fed mice, Nutr. Metab. 8 (2011) 51, https://doi.org/10.1186/1743-7075-8-51.
[47] Q. Wang, S.-L. Ding, Y. Li, J. Royall, D. Feng, P. Lesnar, N. Graddis, M. Naeemi, B. Facer, A. Ho, T. Dolbeare, B. Blanchard, N. Dee, W. Wakeman, K.E. Hirokawa, A. Szafer, S.M. Sunkin, S.W. Oh, A. Bernard, J.W. Phillips, M. Hawrylycz, C. Koch, H. Zeng, J.A. Harris, L. Ng, The Allen Mouse Brain Common Coordinate Framework: A 3D Reference Atlas, Cell 181 (2020) 936–953.e20, https://doi.org/10.1016/j.cell.2020.04.007.
[48] S. Bolte, F.P. Cordelières, A guided tour into subcellular colocalization analysis in light microscopy, J Microsc 224 (2006) 213–232, https://doi.org/10.1111/j.1365-2818.2006.01706.x.
[49] J. Christophe, B. Jeanrenaud, J. Mayer, A.E. Renold, Metabolism in vitro of adipose tissue in obese-hyperglycemic and goldthioglucose-treated mice. I. Metabolism of glucose, J Biol Chem 236 (1961) 642–647.
[50] G. Hollifield, W. Parson, C.R. Ayers, In vitro synthesis of lipids from C-14 acetate by adipose tissue from four types of obese mice, American Journal of Physiology-Legacy Content 198 (1960) 37–38, https://doi.org/10.1152/ajplegacy.1960.198.1.37.
[51] S.A. Sowah, F. Hirche, A. Milanese, T.S. Johnson, M. Grafetstätter, R. Schübel, R. Kirsten, C.M. Ulrich, R. Kaaks, G. Zeller, T. Kühn, G.I. Stangl, Changes in Plasma Short-Chain Fatty Acid Levels after Dietary Weight Loss among Overweight and Obese Adults over 50 Weeks, Nutrients 12 (2020) 452, https://doi.org/10.3390/nu12020452.
[52] Z. Ang, J.L. Ding, GPR41 and GPR43 in Obesity and Inflammation – Protective or Causative? Front. Immunol. 7 (2016) https://doi.org/10.3389/fimmu.2016.00028.
[53] T.M. Becker, M. Favero, V. Di Marzo, L. Cristino, G. Busetto, Endocannabinoid-dependent disinhibition of orexinergic neurons: Electrophysiological evidence in leptin-knockout obese mice, Molecular Metabolism 6 (2017) 594–601, https://doi.org/10.1016/j.molmet.2017.04.005.
[54] M. Pizzonero, S. Dupont, M. Babel, S. Beaumont, N. Bienvenu, R. Blanqué, L. Cherel, T. Christophe, B. Crescenzi, E. De Lemos, P. Delerive, P. Deprez, S. De Vos, F. Djata, S. Fletcher, S. Kopiejewski, C. L'Ebraly, J.-M. Lefrançois, S. Lavazais, M. Manioc, L. Nelles, L. Oste, D. Polancec, V. Quénéhen, F. Soulas, N. Triballeau, E. M. Van Der Aar, N. Vandeghinste, E. Wakselman, R. Brys, L. Saniere, Discovery and Optimization of an Azetidine Chemical Series As a Free Fatty Acid Receptor 2 (FFA2) Antagonist: From Hit to Clinic, J. Med. Chem. 57 (2014) 10044–10057, https://doi.org/10.1021/jm5012885.
[55] X. Ma, L. Zubcevic, J.C. Bruning, F.M. Ashcroft, D. Burdakov, Electrical Inhibition of Identified Anorexigenic POMC Neurons by Orexin/Hypocretin, J. Neurosci. 27 (2007) 1529–1533, https://doi.org/10.1523/JNEUROSCI.3583-06.2007.
[56] R.-G. Xiong, D.-D. Zhou, S.-X. Wu, S.-Y. Huang, A. Saimaiti, Z.-J. Yang, A. Shang, C.-N. Zhao, R.-Y. Gan, H.-B. Li, Health Benefits and Side Effects of Short-Chain Fatty Acids, Foods 11 (2022) 2863, https://doi.org/10.3390/foods11182863.
[57] N.M. Vittoz, C.W. Berridge, Hypocretin/Orexin Selectively Increases Dopamine Efflux within the Prefrontal Cortex: Involvement of the Ventral Tegmental Area, Neuropsychopharmacol 31 (2006) 384–395, https://doi.org/10.1038/sj.npp.1300807.
[58] F. Lai, F. Cucca, R. Frau, F. Corrias, M. Schlich, P. Caboni, A.M. Fadda, V. Bassareo, Systemic Administration of Orexin a Loaded Liposomes Potentiates Nucleus Accumbens Shell Dopamine Release by Sucrose Feeding, Front. Psychiatry 9 (2018) 640, https://doi.org/10.3389/fpsyt.2018.00640.
[59] L. Tunisi, Orexin-A-mediated control of VTA-NAc mesolimbic pathway contributes to hyperphagia and by endocannabinoid 2-AG-mediated disinhibition of dopaminergic neurons, (n.d.).
[60] B.D. Rowlands, M. Klugmann, C.D. Rae, Acetate metabolism does not reflect astrocytic activity, contributes directly to GABA synthesis, and is increased by silent information regulator 1 activation, J. Neurochem. 140 (2017) 903–918, https://doi.org/10.1111/jnc.13916.
[61] Y. Sun, H. Zhang, X. Zhang, W. Wang, Y. Chen, Z. Cai, Q. Wang, J. Wang, Y. Shi, Promotion of astrocyte-neuron glutamate-glutamine shuttle by SCFA contributes to the alleviation of Alzheimer's disease, Redox Biol. 62 (2023) 102690, https://doi.org/10.1016/j.redox.2023.102690.
[62] A. Inagaki, M. Hayashi, N. Andharia, H. Matsuda, Involvement of butyrate in electrogenic K+ secretion in rat rectal colon, Pflugers Arch - Eur, J Physiol 471 (2019) 313–327, https://doi.org/10.1007/s00424-018-2208-y.
[63] L. Macia, J. Tan, A.T. Vieira, K. Leach, D. Stanley, S. Luong, M. Maruya, C. Ian McKenzie, A. Hijikata, C. Wong, L. Binge, A.N. Thorburn, N. Chevalier, C. Ang, E. Marino, R. Robert, S. Offermanns, M.M. Teixeira, R.J. Moore, R.A. Flavell, S. Fagarasan, C.R. Mackay, Metabolite-sensing receptors GPR43 and GPR109A facilitate dietary fibre-induced gut homeostasis through regulation of the inflammasome, Nat Commun 6 (2015) 6734, https://doi.org/10.1038/ncomms7734.
[64] N. Forte, A.C. Fernández-Rilo, L. Palomba, V. Di Marzo, L. Cristino, Obesity Affects the Microbiota–Gut–Brain Axis and the Regulation Thereof by Endocannabinoids and Related Mediators, IJMS 21 (2020) 1554, https://doi.org/10.3390/ijms21051554.
[65] C. Goswami, Y. Iwasaki, T. Yada, Short-chain fatty acids suppress food-intake by activating vagal afferent neurons, J. Nutr. Biochem. 57 (2018) 130–135, https://doi.org/10.1016/j.jnutbio.2018.03.009.
[66] Y. Xiong, N. Miyamoto, K. Shibata, M.A. Valasek, T. Motoike, R.M. Kedzierski, M. Yanagisawa, Short-chain fatty acids stimulate leptin production in adipocytes through the G protein-coupled receptor GPR41., Proceedings of the National Academy of Sciences of the United States of America 101 (2004) 1045–1050. https://doi.org/10.1073/pnas.2637002100.
[67] N. Forte, S. Boccella, L. Tunisi, A.C. Fernández-Rilo, R. Imperatore, F.A. Iannotti, M. De Risi, M. Iannotta, F. Piscitelli, R. Capasso, P. De Girolamo, E. De Leonibus, S. Maione, V. Di Marzo, L. Cristino, Orexin-A and endocannabinoids are involved in obesity-associated alteration of hippocampal neurogenesis, plasticity, and episodic memory in mice, Nat. Commun. 12 (2021) 6137, https://doi.org/10.1038/s41467-021-26388-4.
[68] H. Shi, X. Ge, X. Ma, M. Zheng, X. Cui, W. Pan, P. Zheng, X. Yang, P. Zhang, M. Hu, T. Hu, R. Tang, K. Zheng, X.-F. Huang, Y. Yu, A fiber-deprived diet causes cognitive impairment and hippocampal microglia-mediated synaptic loss through the gut microbiota and metabolites, Microbiome 9 (2021) 223, https://doi.org/10.1186/s40168-021-01172-0.
[69] S. Perna, Z. Ilyas, A. Giacosa, C. Gasparri, G. Peroni, M.A. Faliva, C. Rigon, M. Naso, A. Riva, G. Petrangolini, A.A.A. Redha, M. Rondanelli, Is Probiotic Supplementation Useful for the Management of Body Weight and Other Anthropometric Measures in Adults Affected by Overweight and Obesity with Metabolic Related Diseases? A Systematic Review and Meta-Analysis, Nutrients 13 (2021) 666, https://doi.org/10.3390/nu13020666.
[70] A. Nogal, P. Louca, X. Zhang, P.M. Wells, C.J. Steves, T.D. Spector, M. Falchi, A. M. Valdes, C. Menni, Circulating Levels of the Short-Chain Fatty Acid Acetate Mediate the Effect of the Gut Microbiome on Visceral Fat, Front. Microbiol. 12 (2021) 711359, https://doi.org/10.3389/fmicb.2021.711359.
[71] W. Fusco, M.B. Lorenzo, M. Cintoni, S. Porcari, E. Rinninella, F. Kaitsas, E. Lener, M.C. Mele, A. Gasbarrini, M.C. Collado, G. Cammarota, G. Ianiro, Short-Chain Fatty-Acid-Producing Bacteria: Key Components of the Human Gut Microbiota, Nutrients 15 (2023) 2211, https://doi.org/10.3390/nu15092211.
[72] S. Zhang, Y. Dang, Roles of gut microbiota and metabolites in overweight and obesity of children, Front. Endocrinol. 13 (2022) 994930, https://doi.org/10.3389/fendo.2022.994930.
[73] X. Chen, Q. Kong, X. Zhao, C. Zhao, P. Hao, I. Irshad, H. Lei, M.-F.-A. Kulyar, Z. A. Bhutta, H. Ashfaq, Q. Sha, K. Li, Y. Wu, Sodium acetate/sodium butyrate alleviates lipopolysaccharide-induced diarrhea in mice via regulating the gut microbiota, inflammatory cytokines, antioxidant levels, and NLRP3/Caspase-1 signaling, Front. Microbiol. 13 (2022) 1036042, https://doi.org/10.3389/fmicb.2022.1036042.
[74] P.D. Cani, S. Possemiers, T. Van de Wiele, Y. Guiot, A. Everard, O. Rottier, L. Geurts, D. Naslain, A. Neyrinck, D.M. Lambert, G.G. Muccioli, N.M. Delzenne, Changes in gut microbiota control inflammation in obese mice through a mechanism involving GLP-2-driven improvement of gut permeability, Gut 58 (2009) 1091–1103, https://doi.org/10.1136/gut.2008.165886.
[75] R.A. Bagarolli, N. Tobar, A.G. Oliveira, T.G. Araújo, B.M. Carvalho, G.Z. Rocha, J. F. Vecina, K. Calisto, D. Guadagnini, P.O. Prada, A. Santos, S.T.O. Saad, M.J. A. Saad, Probiotics modulate gut microbiota and improve insulin sensitivity in DIO mice, J. Nutr. Biochem. 50 (2017) 16–25, https://doi.org/10.1016/j.jnutbio.2017.08.006.
[76] A.W. Rautmann, C.B. De La Serre, Microbiota's Role in Diet-Driven Alterations in Food-intake: Satiety, Energy Balance, and Reward, Nutrients 13 (2021) 3067, https://doi.org/10.3390/nu13093067.
[77] M.W. Pfaffl, Relative expression software tool (REST(C)) for group-wise comparison and statistical analysis of relative expression results in real-time PCR, Nucleic Acids Res. 30 (2002) 36e–e, https://doi.org/10.1093/nar/30.9.e36.